

## CLIMATOLOGY

# Unprecedented climate events: Historical changes, aspirational targets, and national commitments

Noah S. Diffenbaugh,<sup>1,2\*</sup> Deepti Singh,<sup>3,4</sup> Justin S. Mankin<sup>3,5,6</sup>

The United Nations Paris Agreement creates a specific need to compare consequences of cumulative emissions for pledged national commitments and aspirational targets of 1.5° to 2°C global warming. We find that humans have already increased the probability of historically unprecedented hot, warm, wet, and dry extremes, including over 50 to 90% of North America, Europe, and East Asia. Emissions consistent with national commitments are likely to cause substantial and widespread additional increases, including more than fivefold for warmest night over ~50% of Europe and >25% of East Asia and more than threefold for wettest days over >35% of North America, Europe, and East Asia. In contrast, meeting aspirational targets to keep global warming below 2°C reduces the area experiencing more than threefold increases to <10% of most regions studied. However, large areas—including >90% of North America, Europe, East Asia, and much of the tropics—still exhibit sizable increases in the probability of record-setting hot, wet, and/or dry events.

## INTRODUCTION

Recognition of the proportional relationship between cumulative carbon emissions and global temperature change represents one of the most important insights of climate science during the past decade (1–3). This proportional relationship, which is seen in both the historical record and climate model simulations (3), has catalyzed a transition to international policy structures that are built around cumulative emissions (4, 5), culminating in the United Nations (UN) Paris Agreement (6). Given the structure of the Paris Agreement, there is a specific need to compare the levels of cumulative emissions identified in the nationally determined contributions (NDCs; which represent the actual country commitments) and the more aspirational targets of “aggregate emission pathways in order to hold the increase in global average temperature to well below 2°C above pre-industrial levels and to limit the temperature increase to 1.5°C above pre-industrial levels” (6).

Differences in the mean climate between the UN cumulative emissions targets and the UN cumulative emissions commitments could be large enough to affect natural and human systems (7). However, for a number of reasons, it is likely that the highest-impact differences between the UN targets and commitments will be driven by differences in the response of extreme events. First, when observing the historical record, it is clear that the most acute climate vulnerabilities are associated with extremes (8–10). These vulnerabilities are seen across human and natural systems, including both wealthy and poor communities, and both terrestrial and marine ecosystems (10). Second, assessments of the potential impacts of future climate change identify changes in the frequency and/or intensity of extremes as a primary driver of future risks (10–13). This is particularly true for smaller increases in climate forcing, where small changes in the mean can create high-impact changes in extremes (14–18). Comparing potential impacts between the UN targets and commitments therefore requires rigorous, observationally based quantification of changes in the likelihood of extremes (19–21).

Changes in various quantiles of extremes have been thoroughly explored (3, 10, 13). However, accurately quantifying the probability that

future events exceed the most extreme value found in the historical record poses unique challenges (22). For example, the magnitudes of many recent record-setting events have been particularly extreme relative to the length of available historical observations. The limited observational sample, combined with the nonstationarity of the historical time series, creates numerous challenges for quantifying the true underlying variability and hence the true probability of the record event (23). Likewise, if the UN’s aspirational targets are to be achieved, then emissions will need to be dramatically reduced over the near-term decades (24). Those near-term decadal time scales exhibit substantial ambiguity between the signal of climate forcing and the noise of climate variability, particularly on the regional and local scales at which extreme events occur (22, 25–27).

Despite these methodological challenges, the distinct risks posed by unprecedented events create a pressing need to quantify their probabilities at cumulative emissions levels consistent with the UN targets and commitments. We therefore extend the methods of Diffenbaugh *et al.* (22), who developed multiple metrics for testing the influence of global warming on the severity and probability of historically unprecedented events. However, whereas Diffenbaugh *et al.* focused exclusively on the historical period using a single climate model, we extend their methods to quantify the probability of record-setting hot, cold, wet, and dry extremes at all available observational grid points, using multiple climate models, for both historical climate forcing and future forcing windows. These future forcing windows are selected to be consistent with global warming of ~1° to 2°C and ~2° to 3°C, allowing us to quantify the differing risks of unprecedented climate extremes associated with the UN aspirational targets versus the UN NDC commitments (28).

Although numerous studies and assessments have examined the response of extreme events to changes in climate forcing (19, 29–31), our analyses expand on these previous efforts in a number of ways. First, we compare the influence of human forcing on the probability of unprecedented extremes for multiple metrics, both during the historical period and for future periods consistent with the UN cumulative emissions budgets. This comparison enables quantification of the level of adaptation—in terms of increased climate risk—that will be required if different targets are achieved and of the value—in terms of avoided climate risk—associated with different levels of emissions mitigation.

Second, previous analyses of changes in extreme events have been largely confined to changes in simulated quantile thresholds, which

Copyright © 2018  
The Authors, some  
rights reserved;  
exclusive licensee  
American Association  
for the Advancement  
of Science. No claim to  
original U.S. Government  
Works. Distributed  
under a Creative  
Commons Attribution  
NonCommercial  
License 4.0 (CC BY-NC).

<sup>1</sup>Department of Earth System Science, Stanford University, Stanford, CA 94305, USA.

<sup>2</sup>Woods Institute for the Environment, Stanford University, Stanford, CA 94305, USA.

<sup>3</sup>Lamont-Doherty Earth Observatory of Columbia University, Palisades, NY 10964, USA. <sup>4</sup>School of the Environment, Washington State University, Vancouver, WA 98686, USA. <sup>5</sup>NASA Goddard Institute for Space Studies, New York, NY 10025, USA.

<sup>6</sup>Department of Geography, Dartmouth College, Hanover, NH 03755, USA.

\*Corresponding author. Email: diffenbaugh@stanford.edu

often do not represent the record-setting event (19, 29–31). Our analyses provide a new quantification of uncertainty in the probability of unprecedented events that is grounded in the observed historical statistics of multiple extreme climate metrics. Because the UN emissions budgets span overlapping uncertainty in global temperature change (28), this observationally based treatment of uncertainty is particularly critical for quantifying differences in unprecedented event probabilities between the UN targets and commitments.

## RESULTS

The CLIMDEX project has archived a suite of globally gridded observed and simulated extreme event indices (29, 32). We analyze eight of the CLIMDEX indices, which together provide two metrics

each for hot, cold, wet, and dry extremes [Fig. 1 and fig. S1; see Materials and Methods for descriptions of the observations and Coupled Model Intercomparison Project (CMIP5) simulations].

Across the eight extreme indices, the probability of the warmest night exhibits the most widespread response to increasing forcing, with almost half of the global-scale return interval ratios exceeding 5 for cumulative emissions consistent with 2° to 3°C of global warming (Fig. 1B). [In this case, a ratio of 5 means that cumulative emissions of ~3500 gigatons (GT) of CO<sub>2</sub> increase the probability of exceeding the historical maximum warmest night by a factor of 5 relative to the world without human influence.] The hottest day, mildest cold night, and mildest freeze length also exhibit substantial sensitivity, with approximately a quarter of the global-scale return interval ratios exceeding 5 for cumulative emissions consistent with 2° to 3°C (Fig. 1, A, C, and D).

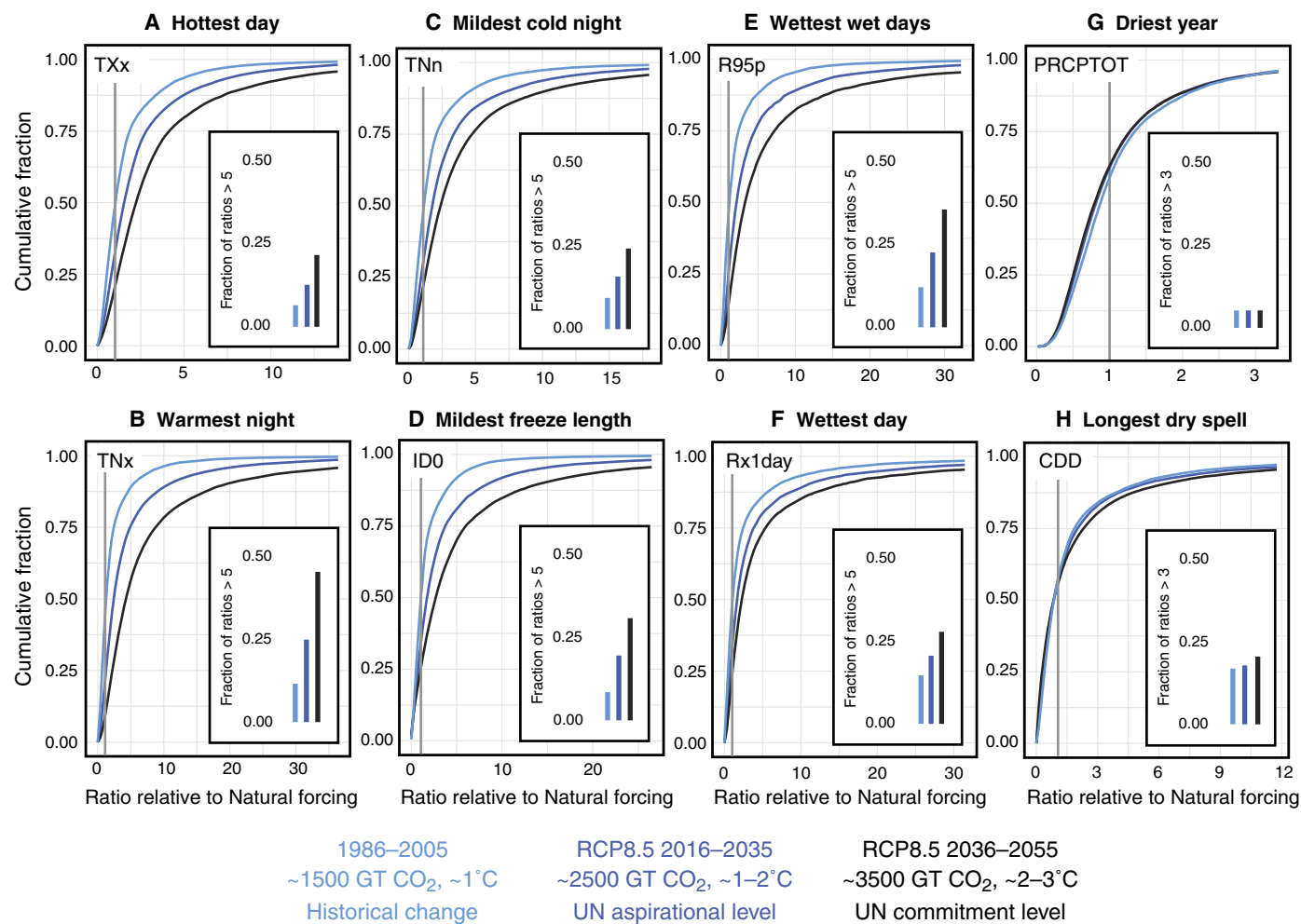


**Fig. 1. The global change in probability of exceeding the historically unprecedented event at three levels of forcing.** Global-scale cumulative distribution functions (CDFs) are calculated from all bootstrapped return interval ratios at all observationally available grid points for each level of anthropogenic forcing (see Materials and Methods). The horizontal axis is the change in probability calculated as the return interval ratio between the natural and anthropogenic forcing. For example, a ratio of 5 means that, in the anthropogenic forcing, the probability of exceeding the most extreme historically observed value is five times the probability in the world without human influence. The vertical axis is the cumulative fraction of all ratios calculated at all available grid points that are less than or equal to a given ratio. Insets show 1 minus the value on the vertical axis, which gives the fraction of ratios that are greater than a given ratio. For example, if a given CDF curve intersects 5 on the horizontal axis and 0.75 on the vertical axis, then 75% of all calculated return interval ratios are less than or equal to 5, and the inset will show that 25% of all calculated ratios are greater than 5. The dark gray vertical line in each panel shows where the return interval ratio between the natural and anthropogenic forcing is equal to 1, meaning that the probability of exceeding the most extreme historically observed value is equivalent in the natural and anthropogenic forcing. The three levels of anthropogenic forcing are the 1986–2005 period of the Historical simulations (~1500 GT CO<sub>2</sub> emitted and ~1°C of global warming above the pre-industrial), the 2016–2035 period of the RCP8.5 simulations (~2500 GT CO<sub>2</sub> and ~1° to 2°C), and the 2036–2055 period of the RCP8.5 simulations (~3500 GT CO<sub>2</sub> and ~2° to 3°C).

Wet events show more widespread sensitivity than dry events, with more than a quarter of the global-scale return interval ratios exceeding 5 for both extreme wet metrics (wettest day and wettest wet days) for cumulative emissions consistent with 2° to 3°C (Fig. 1, E and F). In contrast, although both the driest year and the longest dry spell already exhibit increases in probability in the current climate, they exhibit little additional increase in global extent for cumulative emissions consistent with either 1° to 2°C or 2° to 3°C (Fig. 1, G and H).

The historical forcing has already increased the probability of both the hottest day and the warmest night over most of the observational area (Fig. 2, A and D, and fig. S2). For the hottest day, the historical forcing has increased the probability relative to natural forcings (that is, ratios >1) for more than half of the available data points in East Asia (56.3%), more than two-thirds in North America (70.9%), and more than three-quarters in Europe (76.7%), Australia (82.4%), and southern South America (85%). The historical increases are even more widespread for the warmest night, with ≥90% of the available data points in North

America, Europe, Australia, and southern South America exhibiting ratios of >1, and almost 10% in East Asia exhibiting ratios of >3. Exceeding 2°C of global warming increases the probability of the hottest day substantially. For example, whereas less than 10% of the available data points in Europe exhibit hottest day ratios of >3 (relative to Historical) for cumulative emissions consistent with 1° to 2°C of global warming, more than half (51.7%) exhibit ratios of >3 for cumulative emissions consistent with 2° to 3°C. Similarly, in East Asia, the median hot day ratio remains below 3 (relative to Historical) for all available data points for cumulative emissions consistent with 1° to 2°C of global warming, but more than a quarter of those data points (28.6%) exhibit ratios of >3 for cumulative emissions consistent with 2° to 3°C.

The probability that the coldest events of the year become more mild also increases substantially as cumulative emissions increase (Fig. 3). Most of high-latitude Eurasia and North America have already experienced increased probability that the coldest night of the year exceeds the mildest value on record (Fig. 3A). These increases in probability intensify

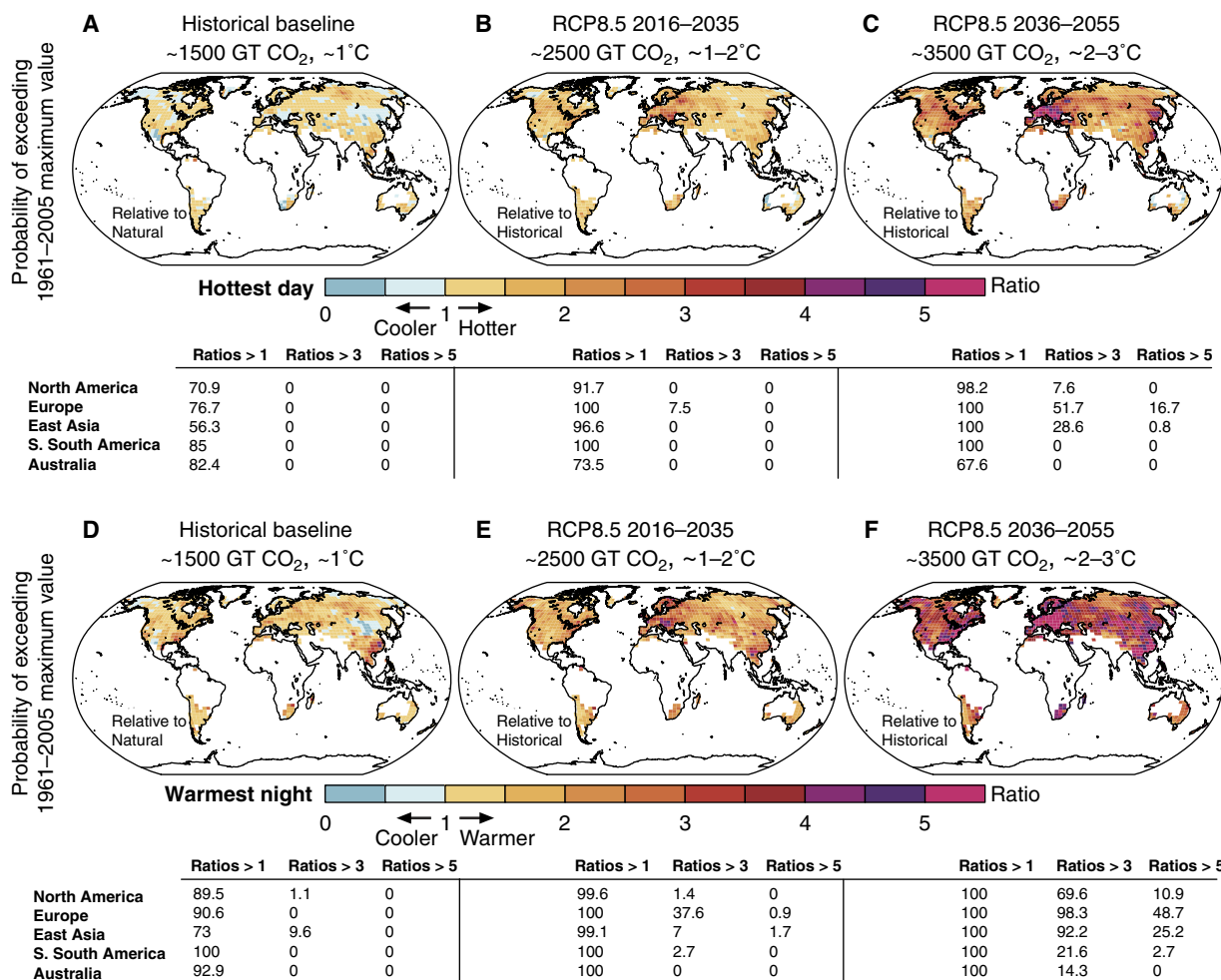


**Fig. 2. The change in probability of exceeding the historically unprecedented hot event at three levels of forcing.** Maps show the median value of the bootstrapped return interval ratios between the lower and higher forcing. (Full distributions for all grid points are shown in Fig. 1). For ratios reported as “relative to Natural,” the lower forcing is that for a world without human influence; for ratios reported as “relative to Historical,” the lower forcing is the combined human and natural forcing that occurred during the historical period (see Materials and Methods). (A to C) Median return interval ratio for the hottest maximum daily temperature of the year (maximum Tx value; “hottest day”). (D to F) Median return interval ratio for the warmest minimum daily temperature of the year (maximum TNx value; “warmest night”). As described in Materials and Methods, the analysis is limited to the areas with observed values in the CLIMDEX data set (missing areas shown in white; fig. S1). See fig. S2 for regional boundaries used in the regional summary calculations.

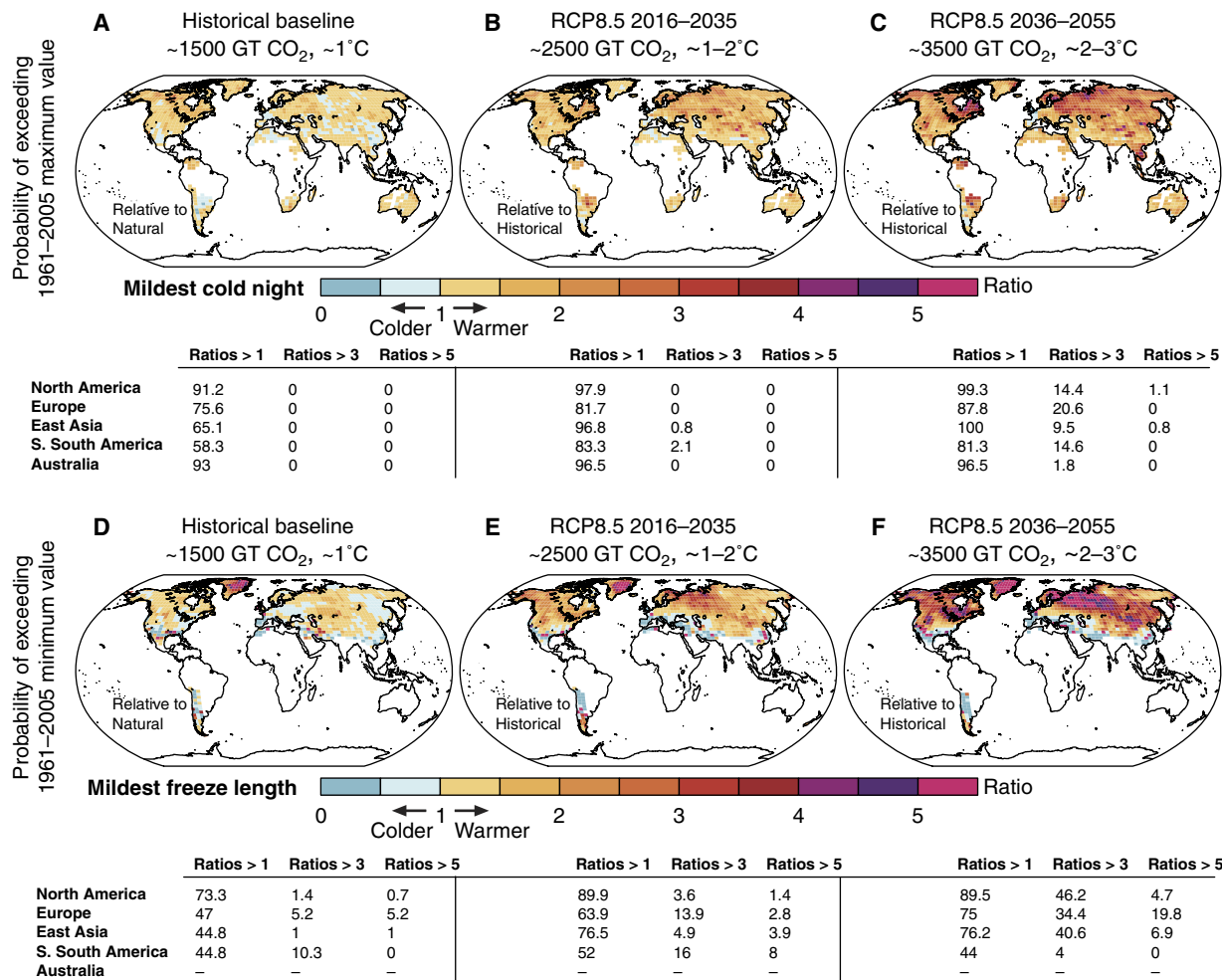


**Fig. 3. The change in probability of exceeding the historically unprecedented mild cold event at three levels of forcing.** As in Fig. 2, but for coldest minimum daily temperature of the year (maximum TN<sub>n</sub> value; “mildest cold night”) and number of days with maximum temperature below 0°C (minimum ID<sub>0</sub> value; “mildest freeze length”).

at higher levels of forcing, with return interval ratios of >2 (relative to Historical) for cumulative emissions consistent with 1° to 2°C of global warming (Fig. 3B), and ratios of >3 for cumulative emissions consistent with 2° to 3°C (Fig. 3C). Areas of high-latitude Eurasia and North America also exhibit particularly strong increases in the probability of the mildest freeze length, including return interval ratios of >4 (relative to Historical) over large areas of Eurasia for cumulative emissions consistent with 2° to 3°C (Fig. 3F).

As with temperature extremes, large fractions of the observed area already exhibit increased probability of record-level wet events, including ≥70% of the available data points in North America, Europe, East Asia, southern South America, and Australia for both extreme wet metrics (Fig. 4, A and D). The fraction of available points that exhibit increases in probability of record-level wet events expands for cumulative emissions consistent with 1° to 2°C of global warming (Fig. 4, B and E). However, the intensification of wet event probability is substantially greater for cumulative emissions consistent with 2° to 3°C, with 15 to 60% of the available data points in North America, Europe, East Asia, and southern South America exhibiting ratios of >3 (relative to Historical) for both metrics (Fig. 4, C and F). We note that the increases in probability are generally more substantial and widespread for the

fraction of total precipitation falling in wet days (“wettest wet days”) than for the magnitude of the wettest single day of the year (“wettest day”). This difference suggests that the risk of increasing extreme wet events is greater than what is indicated by the wettest single event and can occur across a broader range of the precipitation distribution—and therefore potentially result in more sustained wet conditions.

Compared with hot, cold, and wet events, increases in extreme dry probabilities are less widespread (Figs. 1 and 5). This discrepancy is caused primarily by the fact that substantial areas experience decreasing probability of both the driest year and the longest dry spell (Fig. 5). These areas of decreasing dry probabilities are concentrated in the high latitudes, where precipitation increases are most robust (33). However, the fact that continued increases in cumulative emissions do not cause substantial increases in extreme dry probabilities at the global scale (Fig. 1) does not mean that the probability of dry events is not responsive to increasing forcing. Large fractions of the northern and southern hemisphere mid-latitudes exhibit increasing probability of eclipsing the historically driest year and longest dry spell (Fig. 5). These include many areas that are currently heavily populated and highly vulnerable, such as the Mediterranean, southern Africa, Southeast Asia, and southern South America. Not only have increases in event probability

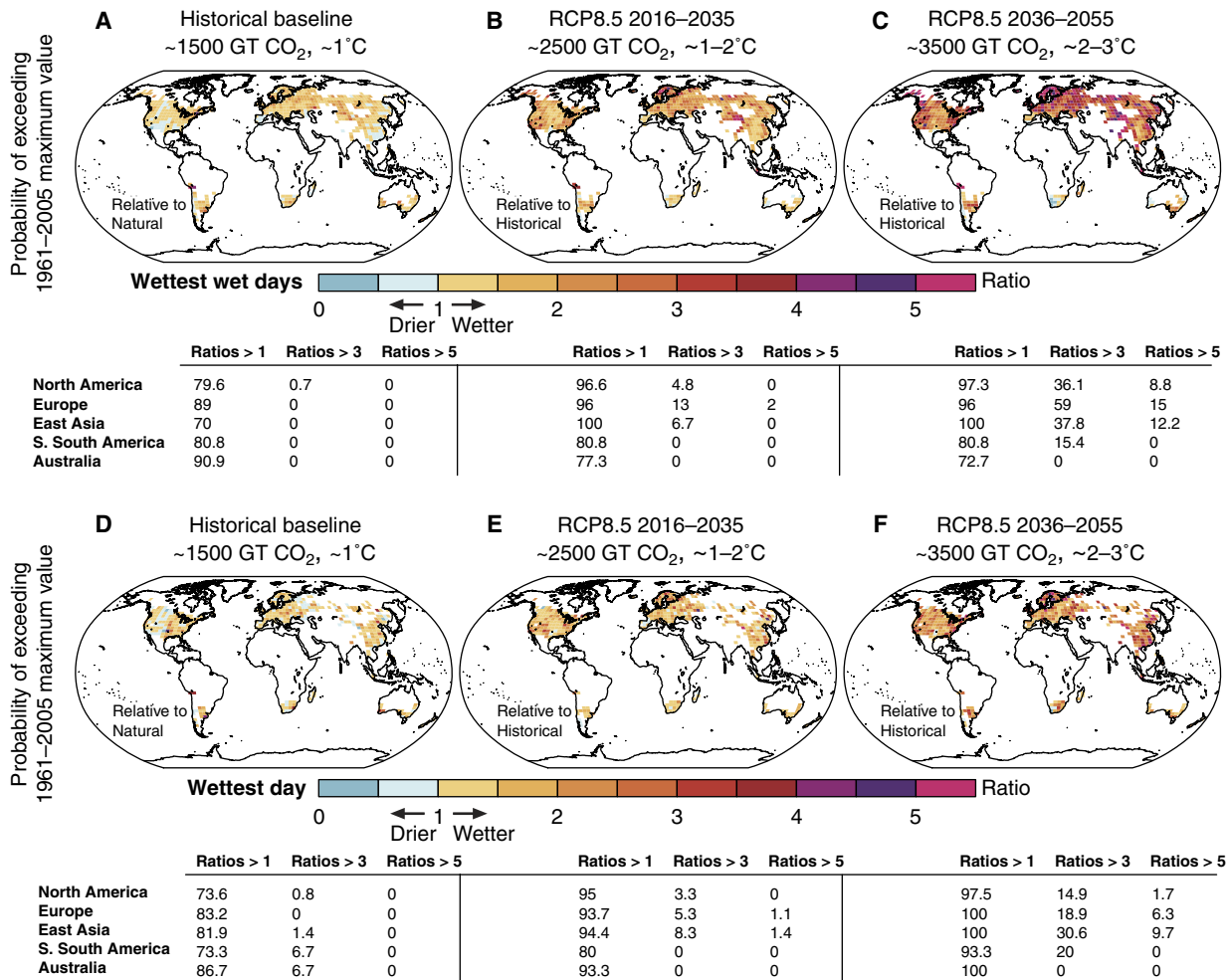


**Fig. 4. The change in probability of exceeding the historically unprecedented wet event at three levels of forcing.** As in Fig. 2, but for annual precipitation from days that exceed the 95th percentile (maximum R95p value; “wettest wet days”) and wettest day of the year (maximum Rx1day value; “wettest day”).

already emerged over most of these regions, but also continued emissions substantially intensify the regional increases. Regional intensification is particularly strong for the longest dry spell, with areas of North America, Europe, southern South America, and southern Africa exhibiting higher probability of record-setting events for cumulative emissions consistent with 2° to 3°C of global warming than 1° to 2°C of global warming (Fig. 5, E and F). The fact that increases in probability are generally more substantial and widespread for the longest dry spell of the year (“longest dry spell”) than for the minimum annual precipitation (“driest year”) suggests that the risk of increasing extreme dry conditions is greater at subannual than annual time scales and that the probability of prolonged dry conditions within the year can increase even if the probability of the driest year does not.

## DISCUSSION

We note a number of important considerations when evaluating our results. One is that although the CMIP5 ensemble accurately simulates the observed variability of most of the extreme indices over most areas, there are areas of disagreement (fig. S1). Although our methodology does use the observed uncertainty in the probability of the record-setting event to implicitly correct errors in the climate model probability

(see Materials and Methods), the regions where the climate model ensemble does not accurately simulate the observed variability (fig. S1) should be treated with caution.

In addition, because our methodology is built around the observed statistics of each extreme climate indicator, analyses are limited to areas with observational coverage in the CLIMDEX data set (22). Areas that lack observational coverage could exhibit substantial changes in the probability of record-setting events, particularly in the tropics, where the mean warming has been large relative to the historical variability (21, 34, 35). Not only would inclusion of these areas alter the global-scale CDFs shown in Fig. 1, but also many of these areas coincide with large human populations, high human vulnerability, and/or high biodiversity, whose exposure to changing extreme event probabilities is not represented in our results due to the lack of observational coverage.

We can provide some estimation of the change in probability in these regions by calculating how often the maximum/minimum value of the CMIP5 natural forcing (“HistoricalNat”) simulations is exceeded in the CMIP5 historical and future scenarios (figs. S3 to S6). These occurrence frequencies suggest that areas lacking observational coverage are also likely to exhibit substantial increases in the probability of events that fall outside of the historical range. For example, for

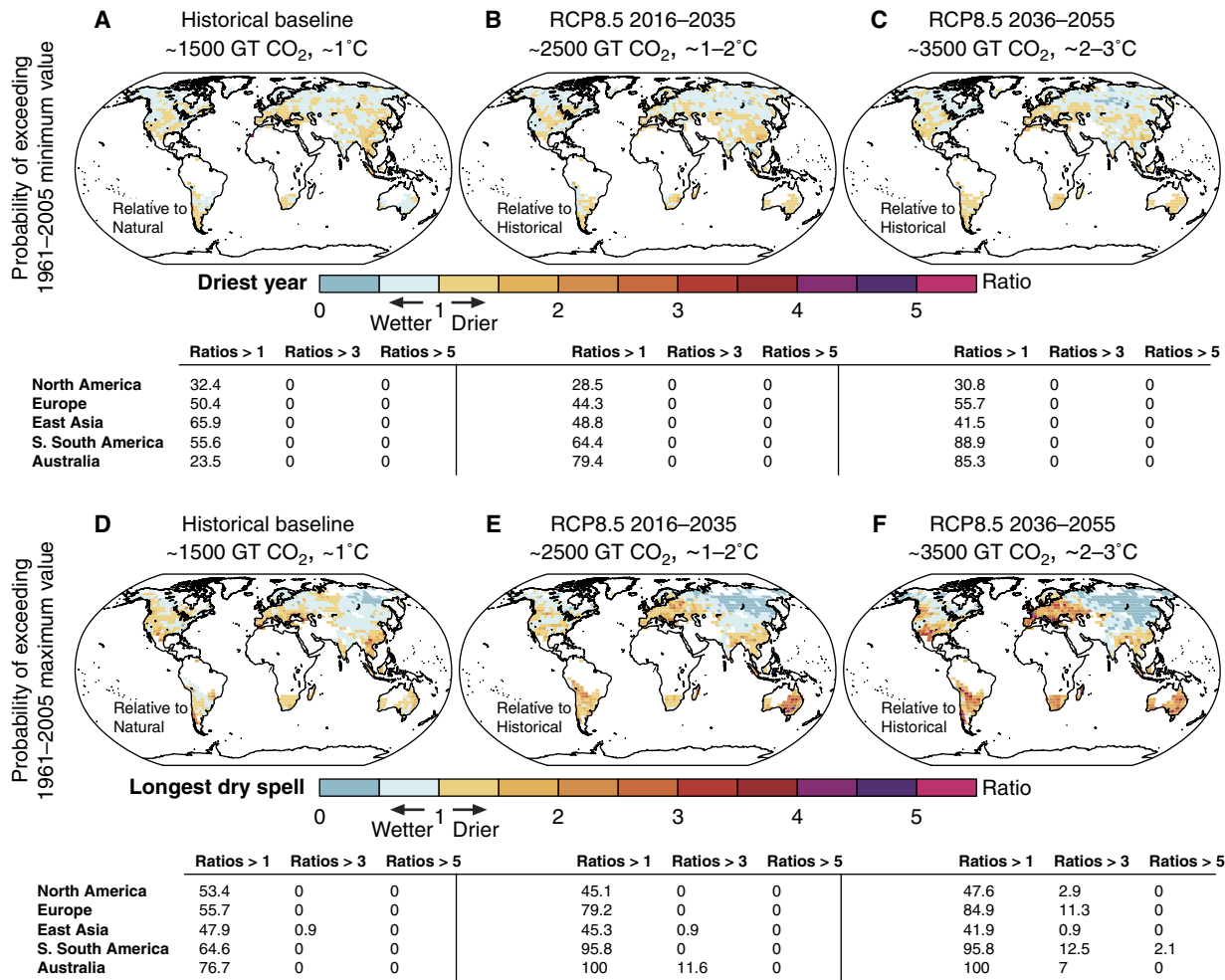


**Fig. 5. The change in probability of exceeding the historically unprecedented dry event at three levels of forcing.** As in Fig. 2, but for total annual precipitation (minimum PRCPTOT value; “driest year”) and longest consecutive dry spell of the year (maximum CDD value; “longest dry spell”).

cumulative emissions consistent with 2° to 3°C of global warming, the occurrence of the hottest day and wettest day is more than five times the recent historical occurrence over most of tropical South America and tropical Africa (figs. S3 and S5). Likewise, for cumulative emissions consistent with both 2° to 3°C and 1° to 2°C, the occurrence of the driest year and longest dry spell is more than three times the recent historical occurrence over substantial fractions of tropical South America and tropical Africa (fig. S6).

We also note that our analysis of cumulative emissions windows within transient climate model simulations is likely to yield conservative estimates of the ultimate climate response, because further regional climate change is likely to occur after emissions are terminated (36). The occurrence frequencies of the maximum/minimum HistoricalNat value in the CMIP5 Representative Concentration Pathway (RCP) simulations (figs. S3 to S6) provide a test of the sensitivity to the pathway of cumulative emissions. For example, the cumulative emissions are similar in RCP8.5 and RCP2.6 in the first three decades of the 21st century, after which they diverge sharply, with the mid-21st century cumulative emissions of RCP8.5 exceeding the late-21st century cumulative emissions of RCP2.6 (3). The rapid decline in annual emissions in RCP2.6 means that the global temperature remains approximately between 1° and 2.5°C above the pre-industrial for the second half of the 21st century of

RCP2.6 (3, 33). Therefore, comparison of the mid-century of RCP2.6 with the late century of RCP2.6 provides an approximation of the sensitivity of the event probability to changes in regional climate that occur after near stabilization of the global temperature. We find that the changes in occurrence between the mid- and late-century of RCP2.6 are broadly similar (figs. S3 to S6). However, a comprehensive quantification of the sensitivity of event probabilities to cumulative emissions pathway will require multiple simulations of multiple stabilization trajectories using multiple climate models.

The conservativeness of our statistical methodology is another reason that our results provide a lower bound on the probability of unprecedented climate events at different levels of forcing identified by global policy-makers. In particular, our methodology selects a parametric distribution that minimizes the return interval ratio (22). Comparing our results with the simple occurrence frequencies in the CMIP5 simulations (figs. S3 to S6) provides a comparison of our probability quantification with the kind of ensemble frequency quantification that has been used in previous studies and assessments (19, 29–31). This comparison shows that our results do exhibit smaller changes than those calculated based on thresholds from the models themselves. However, it should be reiterated that our method allows calculation of the uncertainty in the probability of the actual observed record-setting

event based on the statistics of the observed distribution (22), which is distinct from approaches that have analyzed the frequency of occurrence of the simulated quantiles (19, 29–31).

Our analyses also provide an important comparison with the historical attribution analyses of Diffenbaugh *et al.* (22). First, we extend the number of extreme event metrics from four in the study of Diffenbaugh *et al.* to eight in the current analysis. Second, whereas Diffenbaugh *et al.* did not differentiate human and natural forcings during the historical period, our analysis isolates the human component of the historical climate forcing. Third, whereas Diffenbaugh *et al.* used many realizations of a single climate model [the National Center for Atmospheric Research (NCAR) “Large Ensemble”], our analysis spans a larger range of uncertainty by analyzing results from multiple climate models.

A high priority of the proof-of-concept study of Diffenbaugh *et al.* (22) was to isolate the “irreducible uncertainty” arising from internal climate system variability. In contrast, our emphasis on quantitatively comparing historical and future changes makes spanning both internal variability and model structural uncertainty a key requirement. As shown by Diffenbaugh *et al.*, the historical global warming in the NCAR Large Ensemble falls in the lower half of the CMIP5 multimodel ensemble. Therefore, by using many climate models, our current analysis spans a far greater range of climate sensitivity, which is crucial for comparing climate risks associated with the UN targets versus the UN NDC commitments. Likewise, given the potential for systematic errors in the simulation of the atmosphere and ocean circulation to create errors in the simulated response of temperature and precipitation to changes in forcing (37, 38), the use of multiple climate models also enables our analysis to span a broader range of regional uncertainty.

## CONCLUSIONS

Our results provide the first quantitative comparison of the probability of unprecedented climate events in cumulative emissions windows that are consistent with both historical changes and the UN aspirational targets and pledged national commitments. Analysis of cumulative emissions consistent with global warming of 2° to 3°C shows that the commitments outlined in the UN Paris Agreement are likely to lead to substantial and widespread increases in the probability of historically unprecedented extreme events. For example, 15 to 60% of observed locations in North America, Europe, East Asia, and southern South America exhibit return interval ratios of >3 for most of the extreme indices analyzed here. In contrast, analysis of cumulative emissions consistent with global warming of 1° to 2°C shows that achieving the more aspirational UN targets is likely to substantially limit those increases.

However, even if cumulative emissions are sufficiently constrained to ensure that global warming is held to 1° to 2°C, many areas are still likely to experience substantial increases in the probability of unprecedented events. At the global scale, hot, cold, wet, and dry extremes all exhibit prominent changes in event probability within the 2°C target, including more than fivefold increases at ~25% of the observed area for warmest night and wettest wet days and more than twofold increases at ~25% of the observed area for hottest day. These changes encompass substantial fractions of the United States, Europe, East Asia, and the southern hemisphere mid-latitudes. For example, >90% of observed locations in those regions exhibit increases in the probability of record-hot days and/or record-warm nights relative to the current climate, and 45 to 100% exhibit increases in probability of the longest dry spell. Further, although much of the tropics lack long-term observational

coverage, analyses of climate simulations indicate increases in record hot, wet, and dry events that are at least as substantial as the increases seen over the mid-latitude regions.

Together, our results suggest that the aspirational UN emissions targets are likely to yield substantial reductions in climate risk relative to the changes arising from pledged national commitments but also that those aspirational targets are likely to produce substantial—and potentially high-impact—increases in the probability of unprecedented extremes relative to the current climate.

## MATERIALS AND METHODS

### Observations and models

The CLIMDEX project has archived globally gridded extreme event indices for both historical observations and climate model simulations of historical and future forcing trajectories (29, 32). We analyzed eight of the CLIMDEX indices: (i) hottest maximum daily temperature of the year (TXx), (ii) warmest minimum daily temperature of the year (TNx), (iii) coldest minimum daily temperature of the year (TNn), (iv) number of days with maximum temperature below 0°C (ID0), (v) annual precipitation from days that exceed the 95th percentile (R95p), (vi) wettest day of the year (Rx1day), (vii) total annual precipitation (PRCPTOT), and (viii) longest consecutive dry spell of the year (CDD).

We applied the methods of Diffenbaugh *et al.* (22) to calculate the probability of exceeding the most extreme observed value of each of these eight indices. For these indices, “exceeding the most extreme observed value” means hotter than the maximum TXx value (“hottest day”), warmer than the maximum TNx value (“warmest night”), warmer than the maximum TNn value (“mildest cold night”), fewer days than the minimum ID0 value (“mildest freeze length”), wetter than the maximum R95p value (“wettest wet days”), wetter than the maximum Rx1day value (“wettest day”), drier than the minimum PRCPTOT value (“driest year”), and longer than the maximum CDD value (“longest dry spell”).

CLIMDEX calculated the simulated extreme event indices using output from CMIP5 (39). CLIMDEX has archived indices for the CMIP5 Historical, HistoricalNat, and RCP simulations. We analyzed the climate models for which there are matching realizations in the Historical, HistoricalNat, and RCP8.5 simulations. Following the Intergovernmental Panel on Climate Change (IPCC), we used the “r1i1p1” realization from each model (40), yielding a total of 15 realizations from 15 models.

### Analysis

We followed the analysis of Diffenbaugh *et al.* (22), who compared four attribution metrics during the historical period. To extend the historical analysis of Diffenbaugh *et al.* to periods of elevated climate forcing, we focused on their fourth metric, which is the ratio of return intervals at lower and higher levels of climate forcing. (For example, an event that has a probability of 0.01—or a return interval of 100 years—in the lower forcing and a probability of 0.05—or a return interval of 20 years—in the higher forcing has a return interval ratio of 5). To account for uncertainty in the return interval of the observed record-level event, a distribution of return interval ratios was calculated at each grid point. To do so, we block bootstrapped the grid point time series at the lower and higher forcing levels to generate two distributions of return intervals; we then calculated ratios between all combinations of bootstrapped return intervals at lower and higher forcing, yielding a distribution of return interval ratios (22).

Some modifications are necessary to apply the methods of Diffenbaugh *et al.* (22) to the multimodel CMIP5 ensemble under

both historical and elevated levels of forcing. First, because CLIMDEX archived the extreme indices for the CMIP5 HistoricalNat simulations rather than the CMIP5 Pre-Industrial Control simulations, we used the HistoricalNat experiment as the “counterfactual” world without human influence. (The Pre-Industrial Control and HistoricalNat simulations are similar, but whereas the Pre-Industrial Control simulations use constant pre-industrial forcing, the HistoricalNat simulations add the volcanic and solar forcing that occurred during the historical period; the HistoricalNat simulations therefore enable isolation of the anthropogenic forcing during the historical period). We used the 1961–2005 period to calculate the return interval of the most extreme event in both the observations and the HistoricalNat simulations [see the study of Diffenbaugh *et al.* (22)].

We compared the return interval of the most extreme observed value between the HistoricalNat forcing and three anthropogenic forcing windows: the 1986–2005 period of the Historical simulations, the 2016–2035 period of the RCP8.5 simulations, and the 2036–2055 period of the RCP8.5 simulations. The 1986–2005 period of the Historical simulations is the baseline period used by the IPCC (3, 13), at the end of which there were ~1500 GT CO<sub>2</sub> emitted and ~1°C of global warming above the pre-industrial (3); comparing the return interval of the most extreme observed value between the HistoricalNat simulations and the 1986–2005 period of the Historical simulations quantifies the influence of historical anthropogenic forcing on the probability of the most extreme historical event. The 2016–2035 period of RCP8.5 encompasses a scenario in which there are ~2500 GT CO<sub>2</sub> emitted and ~1° to 2°C of global warming above the pre-industrial (3); comparing the return interval of the most extreme observed value between the 1986–2005 period of the Historical simulations and the 2016–2035 period of RCP8.5 thereby quantifies the change in event probability for a future in which the emissions and global warming targets outlined in the Paris Agreement are met. In contrast, the 2036–2055 period of RCP8.5 encompasses a scenario in which there are ~3500 GT CO<sub>2</sub> emitted and ~2° to 3°C of global warming above the pre-industrial (3); comparing the return interval of the most extreme observed value between the 1986–2005 period of the Historical simulations and the 2036–2055 period of RCP8.5 thereby quantifies the change in event probability for a future in which the UN NDC emissions commitments—but not the UN emissions targets—are met (3, 24, 28, 41).

We note that Millar *et al.* (42) have provided a more recent update of the cumulative emissions-temperature relationship shown in the IPCC Fifth Assessment Report (AR5). Because they are based on the same underlying CMIP5 simulations that were used to generate the findings in the IPCC AR5, the cumulative emissions windows are similar between the periods presented here and those by Millar *et al.* For example, the cumulative emissions that Millar *et al.* identify as having a 66% chance of staying below 1.5°C above the pre-industrial fall close to 2030 of RCP8.5, and the cumulative emissions that Millar *et al.* identify as having a 66% chance of staying below 0.6°C above the recent decade occur near 2040 of RCP8.5. Further, the cumulative emissions that Millar *et al.* identify as having a 66% chance of exceeding 1.1°C above the recent decade fall close to 2050 of RCP8.5.

In addition, whereas the proof-of-concept study of Diffenbaugh *et al.* (22) analyzed many realizations of a single climate model, the CLIMDEX archive contains output from many climate models but at most a few realizations of each model. Given the importance of sufficient population size for quantifying the probability of rare events (23), we pooled the CMIP5 realizations, yielding a total of 300 simulated years in each 20-year forcing period. We found that the pooled climate model output

generally agrees with the CLIMDEX observational data (that is, the *P* value using the Anderson-Darling test comparing distributions is >0.10, indicating that the null hypothesis that the simulated and observed values are drawn from the same underlying distribution cannot be rejected at the 1, 5, or 10% significance levels; fig. S1).

Note that the method of Diffenbaugh *et al.* (22) includes a bias correction step. As described by Diffenbaugh *et al.*, to evaluate each model’s simulation of interannual variability in each climate index, this bias correction is based on the differences between the detrended observations and the climate simulation without human forcings. First, the climate model mean is corrected to be equal to the observational mean (that is, by subtracting the difference between the climate model mean and the observational mean from the climate model time series). In the current analysis, we corrected each CMIP5 realization individually and then pooled the corrected data into a single “bias-corrected” CMIP5 population. This approach allows us to leverage the variability across the full CMIP5 ensemble while simultaneously controlling for the mean biases of the individual climate models. In addition, the method of Diffenbaugh *et al.* also controls for errors in the climate model variability by defining the simulated sample of event return intervals to be identical to the observed sample of event return intervals. That sample of event return intervals is then used to define the sample of event magnitudes in the pool of climate model simulations. This approach of defining the sample of simulated event magnitudes based on the sample of observed event return intervals helps to control for the effect of variability biases on event magnitudes in the tail of the simulated distribution.

## SUPPLEMENTARY MATERIALS

Supplementary material for this article is available at <http://advances.sciencemag.org/cgi/content/full/4/2/eaao3354/DC1>

- fig. S1. Statistical comparison of observed and simulated climate indices during the historical period.
- fig. S2. Regions used in regional summary calculations.
- fig. S3. Frequency of occurrence of the maximum “HistoricalNat” hot event value in the CMIP5 RCP8.5 and RCP2.6 simulations.
- fig. S4. As in fig. S3, but for mild cold events.
- fig. S5. As in fig. S3, but for wet events.
- fig. S6. As in fig. S3, but for dry events.

## REFERENCES AND NOTES

1. H. D. Matthews, K. Caldeira, Stabilizing climate requires near-zero emissions. *Geophys. Res. Lett.* **35**, L04705 (2008).
2. H. D. Matthews, N. P. Gillett, P. A. Stott, K. Zickfeld, The proportionality of global warming to cumulative carbon emissions. *Nature* **459**, 829–832 (2009).
3. Intergovernmental Panel on Climate Change, IPCC, 2013: *Summary for Policymakers in Climate Change 2013: The Physical Science Basis. Contribution of Working Group I to the Fifth Assessment Report of the Intergovernmental Panel on Climate Change* (Cambridge Univ. Press, 2013).
4. K. Zickfeld, M. Eby, H. D. Matthews, A. J. Weaver, Setting cumulative emissions targets to reduce the risk of dangerous climate change. *Proc. Natl. Acad. Sci. U.S.A.* **106**, 16129–16134 (2009).
5. G. P. Peters, R. M. Andrew, S. Solomon, P. Friedlingstein, Measuring a fair and ambitious climate agreement using cumulative emissions. *Environ. Res. Lett.* **10**, 105004 (2015).
6. United Nations Framework Convention on Climate Change, *Adoption of the Paris Agreement* (United Nations Framework Convention on Climate Change, 2015).
7. R. Winkelmann, A. Levermann, A. Ridgwell, K. Caldeira, Combustion of available fossil fuel resources sufficient to eliminate the Antarctic Ice Sheet. *Sci. Adv.* **1**, e1500589 (2015).
8. D. R. Easterling, G. A. Meehl, C. Parmesan, S. A. Changnon, T. R. Karl, L. O. Mearns, Climate extremes: Observations, modeling, and impacts. *Science* **289**, 2068–2074 (2000).

9. C. Parmesan, T. L. Root, M. R. Willig, Impacts of extreme weather and climate on terrestrial biota. *Bull. Am. Meteorol. Soc.* **81**, 443–450 (2000).
10. IPCC, *Managing the Risks of Extreme Events and Disasters to Advance Climate Change Adaptation* (Cambridge Univ. Press, 2012).
11. M. A. White, N. S. Diffenbaugh, G. V. Jones, J. S. Pal, F. Giorgi, Extreme heat reduces and shifts United States premium wine production in the 21st century. *Proc. Natl. Acad. Sci. U.S.A.* **103**, 11217–11222 (2006).
12. D. S. Battisti, R. L. Naylor, Historical warnings of future food insecurity with unprecedented seasonal heat. *Science* **323**, 240–244 (2009).
13. IPCC, Summary for policymakers, in *Climate Change 2014: Impacts, Adaptation, and Vulnerability. Part A: Global and Sectoral Aspects. Contribution of Working Group II to the Fifth Assessment Report of the Intergovernmental Panel on Climate Change*, C. B. Field, V. R. Barros, D. J. Dokken, K. J. Mach, M. D. Mastrandrea, T. E. Bilir, M. Chatterjee, K. L. Ebi, Y. O. Estrada, R. C. Genova, B. Girma, E. S. Kissel, A. N. Levy, S. MacCracken, P. R. Mastrandrea, L. L. White, Eds. (Cambridge Univ. Press, 2014), pp. 1–32.
14. N. S. Diffenbaugh, M. A. White, G. V. Jones, M. Ashfaq, Climate adaptation wedges: A case study of premium wine in the western United States. *Environ. Res. Lett.* **6**, 024024 (2011).
15. N. S. Diffenbaugh, T. W. Hertel, M. Scherer, M. Verma, Response of corn markets to climate volatility under alternative energy futures. *Nat. Clim. Change* **2**, 514–518 (2012).
16. N. S. Diffenbaugh, D. L. Swain, D. Touma, Anthropogenic warming has increased drought risk in California. *Proc. Natl. Acad. Sci. U.S.A.* **112**, 3931–3936 (2015).
17. R. M. Horton, J. S. Mankin, C. Lesk, E. Coffel, C. Raymond, A review of recent advances in research on extreme heat events. *Curr. Clim. Chang. Rep.* **2**, 242–259 (2016).
18. D. Singh, M. Tsiang, B. Rajaratnam, N. S. Diffenbaugh, Precipitation extremes over the continental United States in a transient, high-resolution, ensemble climate model experiment. *J. Geophys. Res. Atmos.* **118**, 7063–7086 (2013).
19. S. I. Seneviratne, M. G. Donat, A. J. Pitman, R. Knutti, R. L. Wilby, Allowable CO<sub>2</sub> emissions based on regional and impact-related climate targets. *Nature* **529**, 477–483 (2016).
20. A. Ciavarella, P. Stott, J. Lowe, Early benefits of mitigation in risk of regional climate extremes. *Nat. Clim. Change* **7**, 326–330 (2017).
21. N. S. Diffenbaugh, A. Charland, Probability of emergence of novel temperature regimes at different levels of cumulative carbon emissions. *Front. Ecol. Environ.* **14**, 418–423 (2016).
22. N. S. Diffenbaugh, D. Singh, J. S. Mankin, D. E. Horton, D. L. Swain, D. Touma, A. Charland, Y. Liu, M. Haugen, M. Tsiang, B. Rajaratnam, Quantifying the influence of global warming on unprecedented extreme climate events. *Proc. Natl. Acad. Sci. U.S.A.* **114**, 4881–4886 (2017).
23. W. K. Huang, M. L. Stein, D. J. McInerney, E. J. Moyer, Estimating changes in temperature extremes from millennial scale climate simulations using generalized extreme value (GEV) distributions. *Adv. Stat. Climatol. Meteorol. Oceanogr.* **2**, 79–103 (2016).
24. B. M. Sanderson, B. C. O'Neill, C. Tebaldi, What would it take to achieve the Paris temperature targets? *Geophys. Res. Lett.* **43**, 7133–7142 (2016).
25. E. Hawkins, R. Sutton, The potential to narrow uncertainty in regional climate predictions. *Bull. Am. Meteorol. Soc.* **90**, 1095–1107 (2009).
26. C. Deser, R. Knutti, S. Solomon, A. S. Phillips, Communication of the role of natural variability in future North American climate. *Nat. Clim. Change* **2**, 775–779 (2012).
27. J. S. Mankin, N. S. Diffenbaugh, Influence of temperature and precipitation variability on near-term snow trends. *Clim. Dyn.* **45**, 1099–1116 (2015).
28. J. Rogelj, M. den Elzen, N. Höhne, T. Fransen, H. Fekete, H. Winkler, R. Schaeffer, F. Sha, K. Riahi, M. Meinshausen, Paris Agreement climate proposals need a boost to keep warming well below 2°C. *Nature* **534**, 631–639 (2016).
29. J. Sillmann, V. V. Kharin, F. W. Zwiers, X. Zhang, D. Bronaugh, Climate extremes indices in the CMIP5 multimodel ensemble: Part 2. Future climate projections. *J. Geophys. Res. Atmos.* **118**, 2473–2493 (2013).
30. E. M. Fischer, R. Knutti, Anthropogenic contribution to global occurrence of heavy-precipitation and high-temperature extremes. *Nat. Clim. Change* **5**, 560–564 (2015).
31. M. Collins, R. Knutti, J. Arblaster, J.-L. Dufresne, T. Fichefet, P. Friedlingstein, X. Gao, W. J. Gutowski, T. Johns, G. Krinner, M. Shongwe, C. Tebaldi, A. J. Weaver, M. Wehner, Long-term climate change: Projections, commitments and irreversibility, in *Climate Change 2013: The Physical Science Basis. Contribution of Working Group I to the Fifth Assessment Report of the Intergovernmental Panel on Climate Change*, T. F. Stocker, D. Qin, G.-K. Plattner, M. Tignor, S. K. Allen, J. Boschung, A. Nauels, Y. Xia, V. Bex, P. M. Midgley, Eds. (Cambridge Univ. Press, 2013).
32. J. Sillmann, V. V. Kharin, X. Zhang, F. W. Zwiers, D. Bronaugh, Climate extremes indices in the CMIP5 multimodel ensemble: Part 1. Model evaluation in the present climate. *J. Geophys. Res. Atmos.* **118**, 1716–1733 (2013).
33. N. S. Diffenbaugh, D. A. Stone, P. Thorne, F. Giorgi, B. C. Hewitson, R. G. Jones, G. J. van Oldenborgh, Cross-chapter box on the regional climate summary figures, in *Climate Change 2014: Impacts, Adaptation, and Vulnerability. Part A: Global and Sectoral Aspects. Contribution of Working Group II to the Fifth Assessment Report of the Intergovernmental Panel on Climate Change*, C. B. Field, V. R. Barros, D. J. Dokken, K. J. Mach, M. D. Mastrandrea, T. E. Bilir, M. Chatterjee, K. L. Ebi, Y. O. Estrada, R. C. Genova, B. Girma, E. S. Kissel, A. N. Levy, S. MacCracken, P. R. Mastrandrea, L. L. White, Eds. (Cambridge Univ. Press, 2014), pp. 137–141.
34. N. S. Diffenbaugh, M. Scherer, Observational and model evidence of global emergence of permanent, unprecedented heat in the 20th and 21st centuries. *Clim. Change* **107**, 615–624 (2011).
35. I. Mahlstein, R. Knutti, S. Solomon, R. W. Portmann, Early onset of significant local warming in low latitude countries. *Environ. Res. Lett.* **6**, 034009 (2011).
36. N. P. Gillett, V. K. Arora, K. Zickfeld, S. J. Marshall, W. J. Merryfield, Ongoing climate change following a complete cessation of carbon dioxide emissions. *Nat. Geosci.* **4**, 83–87 (2011).
37. M. Ashfaq, C. B. Skinner, N. S. Diffenbaugh, Influence of SST biases on future climate change projections. *Clim. Dyn.* **36**, 1303–1319 (2010).
38. I. R. Simpson, R. Seager, M. Ting, T. A. Shaw, Causes of change in Northern Hemisphere winter meridional winds and regional hydroclimate. *Nat. Clim. Change* **6**, 65–70 (2015).
39. K. E. Taylor, R. J. Stouffer, G. A. Meehl, An overview of CMIP5 and the experiment design. *Bull. Am. Meteorol. Soc.* **93**, 485–498 (2012).
40. IPCC, in *Climate Change 2013: The Physical Science Basis. Contribution of Working Group I to the Fifth Assessment Report of the Intergovernmental Panel on Climate Change* (Cambridge Univ. Press, 2013), pp. 1311–1394.
41. A. A. Fawcett, G. C. Iyer, L. E. Clarke, J. A. Edmonds, N. E. Hultman, H. C. McJeon, J. Rogelj, R. Schuler, J. Alsalam, G. R. Asrar, J. Creason, M. Jeong, J. McFarland, A. Mundra, W. Shi, Can Paris pledges avert severe climate change? *Science* **350**, 1168–1169 (2015).
42. R. J. Millar, J. S. Fuglestvedt, P. Friedlingstein, J. Rogelj, M. J. Grubb, H. D. Matthews, R. B. Skeie, P. M. Forster, D. J. Frame, M. R. Allen, Emission budgets and pathways consistent with limiting warming to 1.5°C. *Nat. Geosci.* **10**, 741–747 (2017).

**Acknowledgments:** We thank Y. Liu for assistance with the data analysis. We thank CLIMDEX for calculating and archiving the observed and simulated extreme event indices. We acknowledge the World Climate Research Programme's Working Group on Coupled Modelling, which is responsible for CMIP, and we thank the climate modeling groups for producing and making available their model output. Computational facilities were provided by Center for Computational Earth and Environmental Science and Stanford Research Computing Center at Stanford University. Lamont contribution #8183. **Funding:** We acknowledge funding support from the School of Earth, Energy & Environmental Sciences and the Woods Institute for the Environment at Stanford University; the Earth Institute and Lamont-Doherty Earth Observatory of Columbia University; and the U.S. Department of Energy. **Author contributions:** N.S.D. designed the analysis, analyzed data, interpreted results, and wrote the paper. D.S. and J.S.M. contributed to the design of the analysis, interpretation of results, and writing of the paper. **Competing interests:** The authors declare that they have no competing interests. **Data and materials availability:** All data needed to evaluate the conclusions in the paper are present in the paper and/or the Supplementary Materials or are available from the CLIMDEX archive.

Submitted 9 July 2017

Accepted 12 January 2018

Published 14 February 2018

10.1126/sciadv.aao3354

**Citation:** N. S. Diffenbaugh, D. Singh, J. S. Mankin, Unprecedented climate events: Historical changes, aspirational targets, and national commitments. *Sci. Adv.* **4**, eaao3354 (2018).